Chapter 2

Time-Distance Helioseismology

2.1 Solar Oscillations

Solar oscillations were first observed in 1960 by Leighton *et al.* (1960; 1962), who saw ubiquitous vertical motions of the solar photoshere with periods of about 5 minutes and amplitudes of about 1000 m/s. Ten years later, it was suggested that these oscillations might be manifestations of acoustic waves trapped below the photosphere (Ulrich, 1970; Leibacher and Stein, 1971). Deubner (1975) later confirmed this hypothesis by showing that the observed relationship between the spatial and temporal frequencies (see figure 2.1) of the oscillations was close to that predicted by theory. This confirmation marked the birth of helioseismology as a tool for probing the solar interior.

The identification of the solar oscillations with waves trapped in a resonant cavity leads naturally to an analysis in terms of normal modes. In section 2.2 I will briefly describe this formalism and mention some of the earliest helioseismic results. Since this work is concerned with the large-scale dynamics of the Sun, I will describe in slightly more detail the methods used to measure the Sun's internal rotation using a normal mode analysis. After pointing out some of the limitations of this method, section 2.3 will describe the foundations of time-distance helioseismology, the method used in this work, and its application to the measurement of flows.

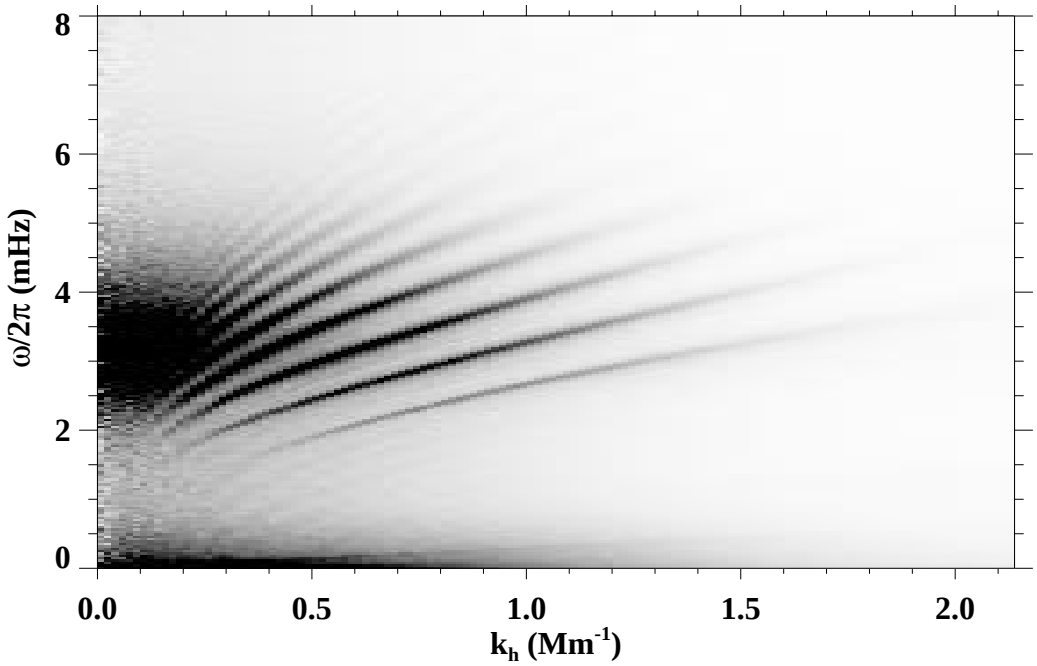

Figure 2.1: The greyscale denotes the power spectrum computed from 8 hours of Dynamics Dopplergrams from MDI. Dark regions are areas of high power. The vertical axis is the temporal cyclic frequency, and the horizontal axis is the horizontal wavenumber. The ridges in the spectrum are regions of resonance which indicate the presence of normal modes of oscillation. The horizontal wavenumber determines the spherical harmonic degree l of the normal mode (see section 2.3.2). The lowest-frequency ridge is the fundamental mode (see section 4.2.3)

2.2 Normal Modes of Oscillation

The Sun forms a resonant cavity for acoustic waves; since the temperature increases with depth, waves which propagate inward from the surface are refracted toward the horizontal and eventually return to the surface. At the surface, they are reflected by the sudden decrease in density. The depth of penetration depends on the horizontal phase speed of the waves.

These oscillations are generally observed by measuring either intensity fluctuations or Doppler motions of the Sun's surface. One way to represent the oscillations is as a

sum of standing waves or normal modes, where the signal observed at a point (r, θ, ϕ) at time t is given by

$$f(r, \theta, \phi, t) = \sum_{nlm} a_{nlm} \xi_{nlm}(r, \theta, \phi) \exp(i[\omega_{nlm} t + \alpha_{nlm}]). \tag{2.1}$$

In this equation, the three integers n, l, and m identify each mode and are commonly called the *radial order*, *angular degree*, and *azimuthal order* respectively. For each mode, a_{nlm} is the mode amplitude, ω_{nlm} is the eigenfrequency, and α_{nlm} is the phase.

The spatial eigenfunction for each mode is denoted by ξ_{nlm}. For a spherically symmetric Sun, the eigenfunctions can be separated into radial and angular components:

$$\xi_{nlm}(r, \theta, \phi) = \xi_{nl}(r) Y_{lm}(\theta, \phi), \tag{2.2}$$

where Y_{lm} is the spherical harmonic and the radial eigenfunction is denoted now by $\xi_{nl}(r)$.

The surface manifestation of solar oscillations can therefore be decomposed into a sum of spherical harmonics for each instant of observation. The result is that the power spectrum of the acoustic signal shows resonant peaks at a particular set of temporal frequencies for each pair (n, l). These peaks identify the eigenfrequencies ω_{nlm} of the normal modes, which can then be used as a diagnostic of the solar interior.

The basic procedure is to identify the eigenfrequencies for a set of normal modes, and then to "invert" these measurements for some property (for example, the sound speed) of the solar interior. In the earliest days of helioseismology, the frequencies were interpreted using simple models and analytical formulae derived from asymptotic analysis. For example, Deubner's measurements implied that the solar convection zone was significantly deeper than predicted by standard models of the day (Gough, 1976). Helioseismology also put an important constraint on the solar helium abundance (Christensen-Dalsgaard and Gough, 1980). More quantitative results were later derived from sophisticated inverse methods.

In a spherically symmetric Sun, all the modes with the same n and l would have the same eigenfrequency ω_{nl}, regardless of the value of $m = \{-l, -l+1, ..., l-1, l\}$. The

Sun, however, is not spherically symmetric, which causes this $(2l+1)$-degeneracy in the frequencies to be broken. This splitting of the frequencies is the basis for helioseismic measurements of the solar internal rotation.

2.2.1 Measuring rotation with mode frequencies

The most obvious symmetry breaker is rotation about a fixed axis. The Sun's rotation causes a splitting of the m-degeneracy in frequency which can be described by

$$\Delta\omega_{nlm} = m \int K_{nlm}(r,\theta)\Omega(r,\theta)\, r\, dr\, d\theta \tag{2.3}$$

Here $\Omega(r,\theta)$ is the angular velocity in the solar interior, $\Delta\omega_{nlm}$ is the frequency difference between the rotating and non-rotating case, and the rotation kernel $K_{nlm}(r,\theta)$ is a weighting function which describes the sensitivity of the mode (n,l,m) to different regions of the solar interior. The kernels are determined by the structure of the eigenfuntions $\xi_{nlm}(r,\theta,\phi)$ in equation 2.2.

In practice, the measured frequency splitting as a function of m and l is often parametrized as an expansion in terms of Legendre polynomials[1]

$$\omega'_{lm} \equiv \bar{\omega}(l,m) - \bar{\omega}(l,0) = l \sum_{k=0}^{k_{max}} a_l^k P_k \left(\frac{m}{l}\right). \tag{2.4}$$

In this expansion, the rotation contributes only to the odd-k a-coefficients, whereas the even-k a-coefficients for each l arise from aspherical effects which cannot distinguish east from west (Brown and Morrow, 1987).

2.2.2 Limitations of the global approach

As noted in section 1.2.1, helioseismic measurements of the solar rotation have become incredibly precise. However, there are several ways in which this approach to the problem is somewhat limited.

[1] Other possibilites exist and are also used.

First, the approach is inherently global. This results in a high precision of measurement but is also an important limitation. In equation 2.3, the frequency splitting is shown to be related to the internal angular velocity through the sensitivity kernels K_{nlm}. Because of the symmetry of the mode eigenfunctions, all the kernels K_{nlm} are symmetric about the equatorial plane. Therefore one consequence of the global approach is that the frequency splitting is sensitive only to that part of Ω which is symmetric about the equatorial plane. Furthermore, since the spherical harmonics depend on longitude ϕ only through $e^{im\phi}$, the kernels are also independent of longitude. Any variations in the angular velocity due to, for example, active regions, are therefore hidden.

Second, until recently the resolution in latitude has been somewhat limited. This resolution is basically limited by the value of k_{max} in equation 2.4. Signal-to-noise considerations have meant that most early results from ground-based observations were limited to $k_{max} = 5$; the resulting rotation profile had three independent points in latitude. This limitation has been largely removed with the advent of the GONG network and the SOHO spacecraft, as frequency splittings are now being extracted for larger values of k_{max} (sometimes up to 35). This higher resolution is needed to resolve small-scale structures like the torsional oscillation.

Third, as noted in the previous section, all the spherically asymmetric effects other than rotation — magnetic fields, structural asphericity, and meridional circulation, for example — cause a splitting of the normal mode frequencies which appears in the even a-coefficients of expansion 2.4. Thus, it is impossible to disentangle any one of these effects from the others (Zweibel and Gough, 1995).

2.3 Time-Distance Helioseismology

Solar oscillations are essentially the only tool astronomers have for looking into the interior of the Sun. Naturally, with the successes of helioseismology on global scales, solar physicists were intrigued by the possibilty of probing the solar interior on smaller scales. Some of the earliest work in this area involved measurements of the interaction between acoustic waves and sunspots (Braun et al., 1988). More recently, there has

been a great interest in using propagating waves to measure the meridional circulation and other flows. The local approach hopes to be complementary to the global approach by overcoming some of the limitations outlined in section 2.2.2.

The various local methods all rely on the interaction of traveling acoustic waves with small perturbations to the background state. Although it is not within the scope of this document to describe all of these methods in detail, each one has its own assumptions, advantages, and disadvantages. The time-distance approach, which is the method used in this work, is described here.

2.3.1 Wave travel times

In the time-distance approach to helioseismology the key concept is the notion of wave travel time. Travel time is a familiar concept in geophysics, where waves are generally excited at specific sources which are localized in space and time. On the Sun, the excitation of acoustic waves is stochastic and it is not yet possible to isolate individual sources in space or time[2]. However, as Duvall (1993) postulated, it is still possible to measure wave travel times[3]. This is done by computing the temporal cross covariance of the signal at a point on the solar surface with the signal at another point.

The *cross covariance* function of the oscillation signals f for two points at coordinates $\mathbf{r_1}$ and $\mathbf{r_2}$ on the solar surface is defined as the integral

$$\psi(\tau, \Delta) = \int_0^T f(\mathbf{r_1}, t+\tau) f^*(\mathbf{r_2}, t)\, dt. \tag{2.5}$$

Here Δ is used to denote the angular distance between the two points and T is the total length of the observations. The time delay τ measures the amount that one signal is shifted relative to the other. The difference between ψ and the *cross correlation* function is a difference of normalization. In this work, all the computed

[2] In one case wave generation due to a solar flare has actually been observed directly (Kosovichev and Zharkova, 1998).

[3] A similar idea was proposed in geophysics by Claerbout (1976).

cross covariances have been normalized according to

$$\psi_0(\tau, \Delta) \equiv \frac{\psi(\tau, \Delta)}{\psi(0, 0)} \tag{2.6}$$

where the term in the denominator is computed by setting $\mathbf{r_1} = \mathbf{r_2}$ and $\tau = 0$ in equation 2.5. I will refer to this function as the cross correlation; however, the exact normalization is almost always irrelevant in time-distance helioseismology.

In practice, it is quite time-consuming to compute the cross correlation with the integral in equation 2.5. Fortunately, the correlation theorem (see, for example, Bracewell (1986)) allows us to change the integral into a product in the Fourier domain,

$$\Psi(\omega_\tau, \Delta) = F(\mathbf{r_1}, \omega)\, F^*(\mathbf{r_2}, \omega). \tag{2.7}$$

Here Ψ is used to represent the temporal (τ) Fourier transform of ψ, and F represents the temporal Fourier transform of f. The length T of the observations is assumed to be long compared to any time lag τ of interest. Since Fourier transforms can be computed very efficiently, equation 2.7 provides a relatively fast way to compute cross correlations.

Assuming that the oscillation signal f can be written in the form of equation 2.1, the Fourier transform F of the observed oscillation signal is given by

$$F(\omega, R_\odot, \theta, \phi) = \sum_{nlm} a_{nlm} \xi_{nl}(R_\odot) Y_{lm}(\theta, \phi) e^{-i\alpha_{nlm}} \delta(\omega - \omega_{nlm}). \tag{2.8}$$

Here the solar surface is denoted by $r = R_\odot$. In practice, the power spectrum of solar oscillations is band-limited. For convenience, let us assume that the amplitudes depend on n and l in the following way:

$$\begin{aligned} &\sum_{nlm} a_{nlm} \xi_{nl}(R_\odot) Y_{lm}(\theta, \phi) e^{-i\alpha_{nlm}} \delta(\omega - \omega_{nlm}) = \\ &\quad \sum_{nlm} G_l(\omega_{nl}) Y_{lm}(\theta, \phi) e^{-i\alpha_{nlm}} \delta(\omega - \omega_{nlm}), \end{aligned} \tag{2.9}$$

where

$$G_l^2(\omega) = \sqrt{2l+1}\exp\left(-\frac{(\omega-\omega_0)^2}{\delta\omega^2}\right). \tag{2.10}$$

If I then compute the product in equation 2.7 and perform the inverse Fourier integral, the result is

$$\psi(\tau,\Delta) = \sum_{nl} G_l^2(\omega_{nl}) e^{i\omega_{nl}\tau} \sum_m \sum_{m'} Y_{lm}(\theta_1,\phi_1) e^{i\alpha_{nlm}} Y_{lm'}^*(\theta_2,\phi_2) e^{-i\alpha_{nlm'}}. \tag{2.11}$$

Since the phases are random, I will assume that on average the terms $e^{i(\alpha_{nlm}-\alpha_{nlm'})}$ will tend to cancel, except of course when $m = m'$. In this case, equation 2.11 becomes

$$\psi(\tau,\Delta) = \sum_{nl} G_l^2(\omega_{nl}) e^{i\omega_{nl}\tau} \sum_m Y_{lm}(\theta_1,\phi_1) Y_{lm}^*(\theta_2,\phi_2). \tag{2.12}$$

The addition theorem for spherical harmonics (see for example Jackson (1975)) allows the simplification

$$\psi(\tau,\Delta) = \sum_{nl} G_l^2(\omega_{nl}) e^{i\omega_{nl}\tau} \left(\frac{2l+1}{4\pi}\right) P_l(\cos\Delta), \tag{2.13}$$

where Δ is the distance between the two points (θ_1,ϕ_1) and (θ_2,ϕ_2):

$$\cos\Delta = \cos\theta_1\cos\theta_2 + \sin\theta_1\sin\theta_2\cos(\phi_1-\phi_2), \tag{2.14}$$

and P_l is the Legendre polynomial of order l.

Again following Jackson (1975), I can approximate

$$P_l(\cos\Delta) \simeq J_0\left([2l+1]\sin\frac{\Delta}{2}\right) \simeq \sqrt{\frac{2}{\pi L\Delta}}\cos\left(L\Delta-\frac{\pi}{4}\right), \tag{2.15}$$

where J_0 is the Bessel function of the first kind. I have introduced the new symbol $L \equiv l + 1/2$; these approximations are valid where Δ is small, but $L\Delta$ is large. Then I have

$$\psi(\tau,\Delta) = \sum_{nl} \frac{2}{\sqrt{\pi\Delta}}\exp\left(-\frac{(\omega_{nl}-\omega_0)^2}{\delta\omega^2}\right)\cos(\omega\tau)\cos(L\Delta). \tag{2.16}$$

Now the double sum can be reduced to a convenient sum of integrals if we regroup the modes so that the outer sum is over the ratio $v \equiv \omega/L$ and the inner sum is over ω. I will show in section 2.3.2 that the travel distance Δ of an acoustic wave is determined by the ratio v; Δ is otherwise independent of ω. In this case, given the band-limited nature of the function G, only values of L which are close to $L_0 \equiv \omega_0/v$ will contribute to the sum, and I expand L near the central frequency ω_0:

$$L\Delta \simeq \Delta \left[L(\omega_0) + \frac{\partial L}{\partial \omega}(\omega - \omega_0) \right] = \Delta \left[\frac{\omega_0}{v} + \frac{\omega - \omega_0}{u} \right], \tag{2.17}$$

where $u \equiv \partial\omega/\partial L$. Furthermore, the product of cosines in equation 2.16 can be changed into a sum; one term is

$$\cos\left[\left(\tau - \frac{\Delta}{u} \right) \omega + \left(\frac{1}{u} - \frac{1}{v} \right) \Delta\omega_0 \right], \tag{2.18}$$

and the other term is identical except that τ has been replaced with $-\tau$ (*i.e.* the time lag is negative). The result is that the double sum in equation 2.16 becomes

$$\psi(\tau, \Delta) = \sum_v \frac{2}{\sqrt{\pi\Delta}} \sum_\omega \exp\left(-\frac{(\omega - \omega_0)^2}{\delta\omega^2} \right) \cos\left(\left[\pm\tau - \frac{\Delta}{u} \right] + \left[\frac{1}{u} - \frac{1}{v} \right] \Delta\omega_0 \right). \tag{2.19}$$

The inner sum can be approximated by an integral over ω; it can be shown (see Gradshteyn and Ryzhik (1994)) that

$$\begin{aligned} \int_{-\infty}^{\infty} d\omega \, \exp\left(-\frac{(\omega - \omega_0)^2}{\delta\omega^2} \right) \cos\left(\left[\tau - \frac{\Delta}{u} \right] \omega - \left[\frac{1}{u} - \frac{1}{v} \right] \Delta\omega_0 \right) = \\ \sqrt{\pi\,\delta\omega^2} \exp\left(-\frac{\delta\omega^2}{4} \left[\tau - \frac{\Delta}{u} \right]^2 \right) \cos\left(\omega_0 \left(\tau - \frac{\Delta}{v} \right) \right). \end{aligned} \tag{2.20}$$

The limits $(-\infty, \infty)$ pose no particular problem since the amplitude function G^2 is essentially zero for very large and very small frequencies. Finally, then, the cross correlation can be expressed as

$$\psi(\tau, \Delta) \propto \sum_v \exp\left(-\frac{\delta\omega^2}{4} \left[\tau \pm \frac{\Delta}{u} \right]^2 \right) \cos\left(\omega_0 \left[\tau \pm \frac{\Delta}{v} \right] \right) \tag{2.21}$$

The cross correlation function at any particular distance is thus described by two characteristic times; the *group time*, defined as $\tau_g \equiv \Delta/u$, and the *phase time*, defined as $\tau_p \equiv \Delta/v$. Furthermore, the cross correlation will have two peaks; one near $+\tau_g$, and the other near $-\tau_g$. These two peaks correspond to the two directions of propagation.

A note is necessary here regarding this rather inelegant derivation of equation 2.21. Several assumptions have been made in the derivation which may not be exactly satisfied in the Sun. Furthermore, I will use the final result in regions well outside the range of validity of the small-angle approximation in equation 2.15. However, these difficulties should not obscure the fact that the form of 2.21 gives a very accurate description of the measured cross correlation! Mathematical details aside, this practical consideration was in fact the original justification for the use of this formula in time-distance helioseismology.

In interpreting the phase and group times in the cross correlation, it is necessary to model the propagation of acoustic waves in the Sun. For this work and almost all time-distance results to date, the propagation is modeled with the ray approximation.

2.3.2 The ray approximation

The acoustic waves observed in this work can be considered high-frequency acoustic waves. In most of the region in which these waves are confined, their wavelengths are short compared to the local temperature and density scale heights. In this wavelength regime, the wave propagation can be approximated with ray theory.

Calculating ray paths

Calculation of ray paths (D'Silva and Duvall, 1995; Gough, 1984) begins with the local dispersion relation, which for the Sun can be written as

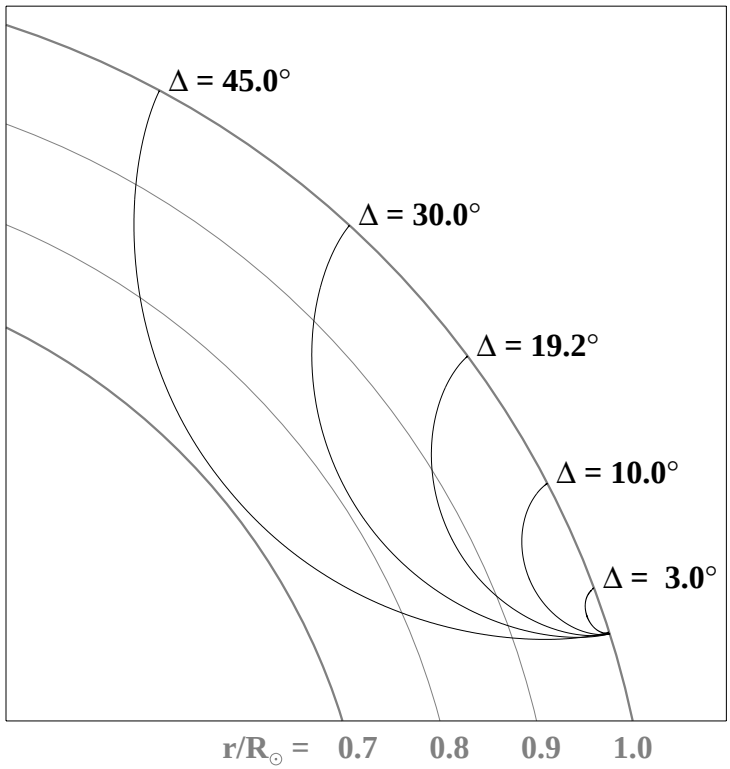

Figure 2.2: A great circle plane containing several sample rays. The grey arcs indicate the fractional radius, and the five black curves show the path taken by waves propagating in the convection zone. The largest ray shown travels a distance of 45° and reaches to $r = 0.71\,\mathrm{R}_\odot$; this is the largest distance for which cross correlations were computed in this work.

$$\begin{aligned} k_r^2 &= \frac{1}{c^2}\left(\omega^2 - \omega_{AC}^2\right) - k_h^2\left(1 - \frac{\omega_{BV}^2}{\omega^2}\right), \\ k_h^2 &= \frac{L^2}{r^2}. \end{aligned} \tag{2.22}$$

The quantity k_h is the horizontal wavenumber; the relation (rk_h = constant) follows from spherical symmetry of the background state. In the modal analysis, it can be shown that $L^2 = l(l+1)$; for large l, $L \simeq (l + 1/2)$ and is the same as the variable L from section 2.3.1.

The symbol k_r denotes the radial wavenumber, c is the sound speed, and the

quantity ω_{BV}, called the Brunt-Väisälä frequency, is given by

$$\omega_{BV}^2 = g\left(\frac{1}{,\ 1}\frac{d\ln p}{dr} - \frac{d\ln\rho}{dr}\right), \tag{2.23}$$

where g is the acceleration due to gravity at radius r. The other characteristic frequency is the acoustic cutoff frequency, for which I use the approximation

$$\omega_{AC}^2 = \frac{c^2}{4H_p^2} \tag{2.24}$$

where H_p is the pressure scale height, defined as

$$H_p = -\left(\frac{d\ln p}{dr}\right)^{-1}. \tag{2.25}$$

The path of an acoustic ray is defined by the equation

$$\frac{dr_p}{r_p\, d\theta_p} = \frac{v_{gr}}{v_{gh}}, \tag{2.26}$$

where the coordinates (r_p, θ_p) describe the path of the ray within a plane containing the center of the Sun. Using the dispersion relation for solar acoustic waves, the radial (v_{gr}) and horizontal (v_{gh}) components of the group velocity can be expressed as

$$\begin{aligned} v_{gr} &\equiv \frac{\partial\omega}{\partial k_r} = \frac{k_r\omega^3c^2}{\omega^4 - k_h^2c^2\omega_{BV}^2}, \\ v_{gh} &\equiv \frac{\partial\omega}{\partial k_h} = k_h\omega c^2\left(\frac{\omega^2-\omega_{BV}^2}{\omega^4 - k_h^2c^2\omega_{BV}^2}\right), \end{aligned} \tag{2.27}$$

In practice, a solar model (Christensen-Dalsgaard et al., 1996) is used to calculate the characteristic frequencies (2.23 and 2.24), and these are used in turn to calculate the horizontal and radial wavenumbers (equation 2.22) and group velocities (2.27). The *turning points* of the ray are defined as those points where the radial wavenumber (and hence the group velocity) goes to zero. Roughly speaking, since $\omega_{BV}^2 \ll \omega^2$ in the convection zone, and $\omega_{AC}^2 \ll \omega^2$ except very near the surface, the upper turning

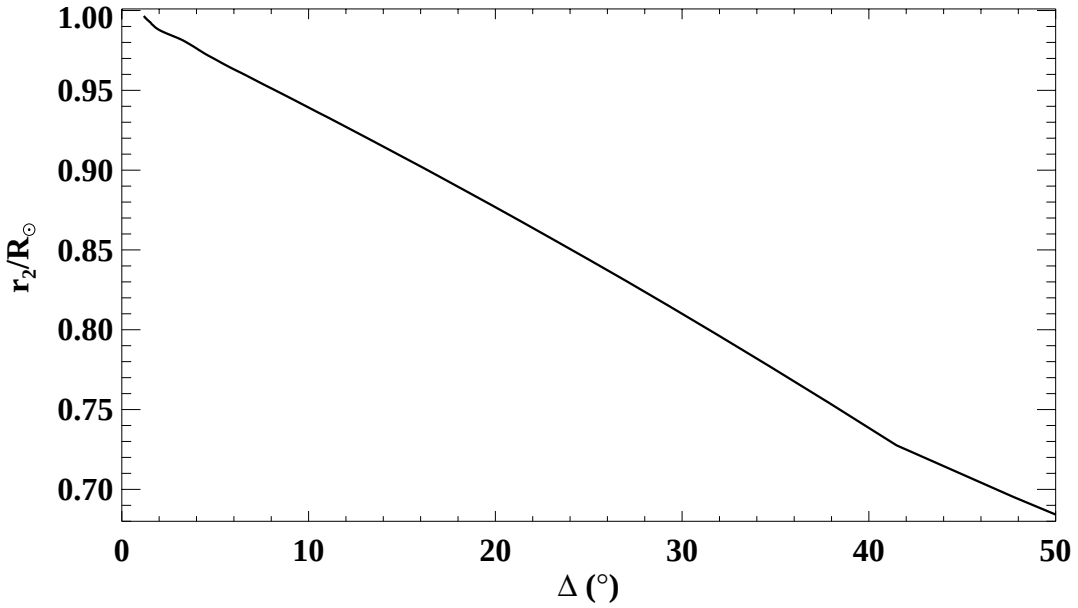

Figure 2.3: The lower turning point r_2 is plotted as a function of the travel distance for acoustic rays with temporal frequency $\omega/2\pi = 3.1\,\mathrm{mHz}$.

point (which I denote by r_1) occurs where $\omega \approx \omega_{AC}$, and the lower turning point (r_2) occurs where $\omega \approx k_h c$. This latter statement leads to the approximate determination of r_2:

$$\frac{c(r_2)}{r_2} \simeq \frac{\omega}{L}. \tag{2.28}$$

This implies that all waves with the same value of ω/L follow the same ray path, a fact that I made use of in section 2.3.1.

Once the turning points have been determined, the angular coordinate θ_p is computed from the integral of equation 2.26:

$$\theta_p(r) = \theta_1 + \int_{r_1}^{r} \frac{v_{gh}(r')}{v_{gr}(r')} \frac{dr'}{r'}, \tag{2.29}$$

where the turning points are defined as (r_1, θ_1) and (r_2, θ_2). Figure 2.2 shows some

sample ray paths. The travel distance of the ray is defined as the angular distance between photospheric reflection points,

$$\Delta \equiv 2|\theta_2 - \theta_1|. \tag{2.30}$$

The relationship between travel distance and turning point depth is shown in figure 2.3. The group travel time can be defined as

$$\tau_g \equiv \int_\Gamma \frac{ds}{v_g} = 2\int_{r_1}^{r_2} \frac{dr}{v_{gr}}, \tag{2.31}$$

where the first integral is a line integral along the ray path (denoted by ,). The phase time can be defined similarly as

$$\tau_p = \int_\Gamma \frac{k\,ds}{\omega} = \int_\Gamma \frac{ds}{v_p}. \tag{2.32}$$

The integrands in equations 2.29, 2.31 and 2.32 are singular at the turning points r_1 and r_2, but the singularities are integrable. For the purposes of numerically performing the integrals, I have used the procedure outlined by Christensen-Dalsgaard *et al.* (1989).

In what follows, I will deal almost exclusively with phase time as defined by equation 2.32. I will leave off the subscript p unless it is ambiguous to do so.

Fermat's Principle

A powerful property of ray paths is that they obey Fermat's Principle, which states that the travel time along the ray is stationary with respect to small changes in the path. This implies that if a small perturbation is made to the background state, the ray path is unchanged.

The perturbation to the travel time can then be expressed as

$$\tau - \tau_0 = \frac{1}{\omega}\int_{\Gamma_0} \delta k\, ds. \tag{2.33}$$

Here δk is the perturbation to the wavevector due to inhomogeneities in the background state, and Fermat's principle allows us to make the integral along the unperturbed ray path , $_0$ (see, for example, Gough (1993)).

In the solar convection zone, the Brunt-Väisälä frequency ω_{BV} is small compared to the acoustic cutoff frequency and the typical frequencies of solar oscillations. Neglecting this frequency, the dispersion relation 2.22 can be written as

$$\begin{aligned} k_r^2 &= \frac{1}{c^2}\left(\omega^2 - \omega_{AC}^2\right) - k_h^2, \\ k_h^2 &= \frac{l(l+1)}{r^2}. \end{aligned} \tag{2.34}$$

If we allow small perturbations (relative to the background state) in ω, c^2, and ω_{AC}^2, then the integrand in equation 2.33 can be written to first order as

$$\frac{\delta k\, ds}{\omega} = \left[\frac{\delta\omega}{c^2 k} - \left(\frac{\delta c}{c}\right)\frac{k}{\omega} - \left(\frac{\delta\omega_{AC}}{\omega_{AC}}\right)\left(\frac{\omega_{AC}^2}{c^2\omega^2}\right)\frac{\omega}{k}\right] ds, \tag{2.35}$$

where I have neglected terms which are second-order in $\delta c/c$ and $|u|/c$.

One possible perturbation to the spherically symmetric background state is a velocity field. If the flow field is described by $\mathbf{u}$ then the observed frequency will be Doppler shifted by the advection of the oscillations,

$$\delta\omega = -k\hat{\mathbf{n}}\cdot\mathbf{u}, \tag{2.36}$$

so that equation 2.33 becomes

$$\tau^{\pm} - \tau_0 = -\int_{\Gamma_0}\left[\frac{\mathbf{u}\cdot(\pm\hat{\mathbf{n}})}{c^2} + \left(\frac{\delta c}{c}\right)\frac{k}{\omega} + \left(\frac{\delta\omega_{AC}}{\omega_{AC}}\right)\left(\frac{\omega_{AC}^2}{c^2\omega^2}\right)\frac{\omega}{k}\right] ds, \tag{2.37}$$

where $\hat{\mathbf{n}}$ is a unit vector tangent to the ray path. Here I have defined the quantity τ^+ as the perturbed travel time in one direction along the ray path (unit vector $+\hat{\mathbf{n}}$) and τ^- as the perturbed travel time in the opposite (reciprocal) direction (unit vector $-\hat{\mathbf{n}}$). To separate the effects of the velocity field from the other perturbations, we

thus define

$$\delta\tau \equiv \tau^+ - \tau^- = -2\int_{\Gamma_0} \frac{\mathbf{u}\cdot\hat{\mathbf{n}}}{c^2}\, ds \tag{2.38}$$

$$\langle\tau\rangle \equiv \frac{(\tau^+ + \tau^-)}{2} = \tau_0 - \int_{\Gamma_0} \left[\left(\frac{\delta c}{c}\right)\frac{k}{\omega} + \left(\frac{\delta\omega_{AC}}{\omega_{AC}}\right)\left(\frac{\omega_{AC}^2}{c^2\omega^2}\right)\frac{\omega}{k}\right] ds. \tag{2.39}$$

Equation 2.38 thus provides the link between the measured travel time differences and the flow field along the ray path. This simple equation will be the heart of the measurements made in this work. The quantities δc and $\delta\omega_{AC}$ contain effects such as perturbations to the temperature and magnetic field[4], which appear in the mean times.

2.3.3 Horizontal and radial flows

Equation 2.38 shows that the time difference $\delta\tau$ for waves traveling on reciprocal ray paths is sensitive to the component of the flow along the ray path. If the radial flow is uniform everywhere, then the net time difference due to the radial velocity will be zero, as reciprocal rays will experience the same net flow. However, it may be the case that the radial component of the velocity is not uniform; imagine a ray path which lies in a meridian plane with a velocity field like the one shown in figure 2.4. This model circulation is horizontal at the surface and satisfies the continuity equation

$$\frac{\partial\rho}{\partial t} + \nabla\cdot(\rho\mathbf{u}) = 0. \tag{2.40}$$

Since the density in the solar convection zone deceases quite rapidly with radius, a meridional circulation which satisfies conservation of mass must have a small radial component.

[4]Strictly speaking, in the presence of a magnetic field the sound speed c should be replaced by the fast magnetoacoustic speed c_f in equation 2.34. See Kosovichev and Duvall (1997) for more details. In this section I am including magnetic effects as perturbations to the quantity c. For further development of the perturbations to the mean times due to magnetic field, see also Ryutova and Scherrer (1998).

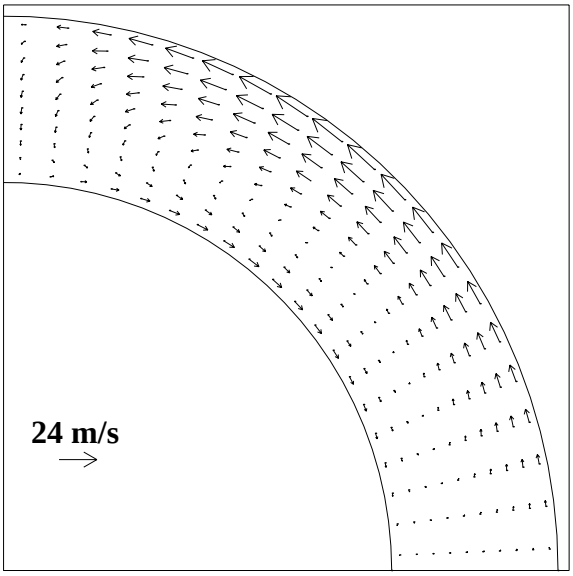

Figure 2.4: A meridional cross section of the solar convection zone. The bottom of the plot represents the equatorial plane. The arrows denote a possible meridional circulation, with the reference length shown in the lower left representing a velocity of 24 m/s. The model shown here satisfies the continuity equation and is horizontal at the solar surface.

We can write the time difference in two components

$$\delta\tau = \delta\tau_h + \delta\tau_r, \tag{2.41}$$

where

$$\delta\tau_h = 2\int_{r_1}^{r_2} \frac{u_h v_{gh}}{v_{gr} c^2} dr, \tag{2.42}$$

$$\delta\tau_r = 2\int_{r_1}^{r_2} \frac{u_r}{c^2} dr. \tag{2.43}$$

Using these equations, it is possible to calculate the relative contributions of the horizontal and radial flows for a selection of latitudes and distances. The results are

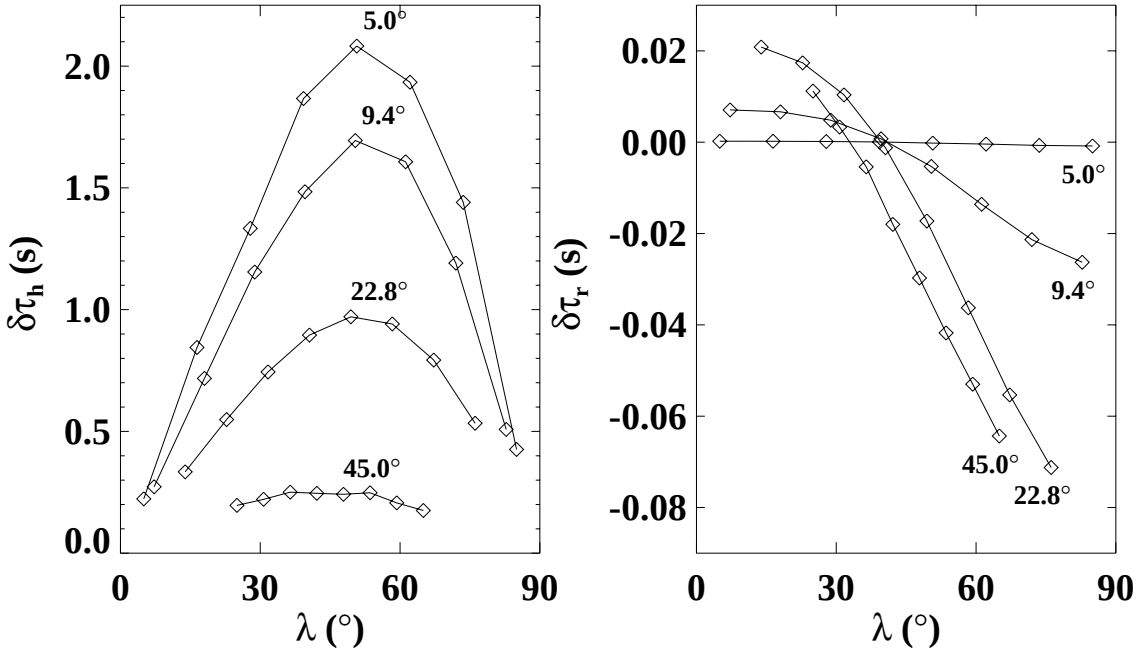

Figure 2.5: The two plots show travel time differences computed using the model in figure 2.4. The left-hand plot shows the time differences due to the horizontal part of the meridional circulation, and the right-hand plot shows the contribution of the radial part of the velocity. The curves in each plot are labelled with their travel distance. Note the different scales in the two plots.

shown in figure 2.5. Since the contribution of the radial flow is always much smaller than the contribution of the horizontal flow, I will always neglect the former; the symbol u will hereafter be used to denote the horizontal flow field. Equation 2.38 can then be replaced by

$$\delta\tau = 2\int_{r_1}^{r_2} \frac{u v_{gh}}{v_{gr} c^2} dr, \tag{2.44}$$

which is used to infer the velocity u from the time differences, as explained in chapter 5.

2.3.4 Wave Effects

Clearly the ray approximation is extremely useful in time-distance helioseismology. However, it is often questioned whether this approximation is entirely justified (see for example Bogdan (1997)). On theoretical grounds, the ray expectation is invalid in the region near the solar surface, where the pressure and density scales vary rapidly. This means that the approximation is worse for very short travel distances where the waves propagate only in the near-surface region. As the travel distance increases, the rays penetrate to depths where the variation of the background is much slower, and the approximation is expected to work quite well.

One important consequence of wave effects is that the travel time is sensitive not only to the local velocity field along the ray path, but also to conditions in the surrounding medium as well. This "broadening" has been clearly demonstrated by Bogdan (1997). In practice, this effect is probably not as important as it might seem at first glance. In almost all time-distance measurements, travel times are averaged over a small range of travel distances and locations. That is, cross correlations are computed for a large number of pairs of points, and then pairs with "similar" distances and locations have their cross correlations averaged together to get a single measurement $\delta\tau$. In interpreting this measurement, then, the ray path used is actually a "ray bundle" consisting of a number of rays covering the region of propagation. The broadening of such a bundle by wave effects might be small compared to the extent of the bundle itself. Some critics of the ray approximation seem to miss this subtlety.

Another possible consequence of wave effects is that the sensitivity along the ray path might be different from that predicted by the ray theory. Some numerical simulations have shown this to be true, with the sensitivity actually being slightly lower along the ray path than in the nearby regions (Birch, 1999). Some work is currently being done to compute more realistic sensitivity functions, using various more general approximations to the wave equation (Jensen et al., 1998). These models will probably play an important role in the future development of time-distance helioseismology.

Finally, let me make the point that ray theory has been used in helioseismology for some time (see, for example, Gough (1984)). The ray approximation is one of several

methods that have been applied to *asymptotic inversions* of helioseismic frequency measurements. In many cases, these analytic methods have been shown to be in very good agreement with more sophisticated numerical techniques which include the full wave nature of the oscillations.

So far, this discussion has glossed over the actual observation and measurement of acoustic wave travel times or even of solar oscillations in general. This question leads to considerations of a more practical nature, which will be expanded in the next two chapters. Chapter 3 describes the MDI instrument and the helioseismic observations it makes. Chapter 4 describes the subsequent analyses which are necessary to extract travel times using the time-distance approach.